Acta Mech 223, 2135–2151 (2012)
DOI 10.1007/s00707-012-0688-y

S. A. Sina · H. Haddadpour · H. M. Navazi

Nonlinear free vibrations of thin-walled beams in torsion

Received: 2 January 2012 / Revised: 13 April 2012 / Published online: 28 June 2012

Abstract Nonlinear torsional vibrations of thin-walled beams exhibiting primary and secondary warpings are investigated. The coupled nonlinear torsional–axial equations of motion are considered. Ignoring the axial inertia term leads to a differential equation of motion in terms of angle of twist. Two sets of torsional boundary conditions, that is, clamped–clamped and clamped-free boundary conditions are considered. The governing partial differential equation of motion is discretized and transformed into a set of ordinary differential equations of motion using Galerkin's method. Then, the method of multiple scales is used to solve the time domain equations and derive the equations governing the modulation of the amplitudes and phases of the vibration modes. The obtained results are compared with the available results in the literature that are obtained from boundary element and finite element methods, which reveals an excellent agreement between different solution methodologies. Finally, the internal resonance and the stability of coupled and uncoupled nonlinear modes are investigated. This study can be a preliminary step in the understanding of complex dynamics of such systems in internal resonance excited by external resonant excitations.

1 Introduction

Thin-walled beams (TWBs) are widely used in engineering applications with minimum weight design criteria, ranging from civil to aerospace and many other industrial fields. Frequently used TWBs have low torsional stiffness, and their torsional deformations may be of such magnitudes that it is not adequate to treat the angles of cross-sectional rotation as small. When the vibration amplitudes are moderate or large, the geometric nonlinearity must be included, and some new phenomena such as hardening (or softening), jump, secondary resonance, etc. come into play [1]. Unfortunately, the equations of motion of nonlinear systems are very complicated, and there are no exact or analytical solutions, in most cases. On the other hand, numerical solutions such as finite element and boundary element methods have no capability to give parametric solutions. Therefore, they cannot be used to investigate the global and qualitative behavior of the system. Some approximate solutions such as perturbation methods can overcome deficiencies of exact and numerical methods.

As a pioneering work in the field of TWB theory, Vlasov [2] used the contour-based cross-sectional analysis with the assumption of small nonuniform angle of twist. The Vlasov's model has been widely used in most theoretical and finite element works on TWBs. Loughlan and Ata [3] studied the effects of primary and secondary warpings on the torsional response of open- and closed-section fiber composite beams. Comparisons between theory, experiment, and finite element solutions are shown to give good agreements for the

S. A. Sina (✉) · H. Haddadpour · H. M. Navazi
Aerospace Engineering Department, Sharif University of Technology,
PO Box: 11365-8639, Azadi Ave., Tehran, Iran
E-mail: sasina@ae.sharif.edu
Tel.: +98-21-66164618
Fax: +98-21-66022720

Z, angle, and box-section beams. Ferrero et al. [4] developed an analytical theory for determining stress and stiffness in a TWB under the twist moment including warping effects. Furthermore, Trahair et al. [5] also used Vlasov's model to investigate the behavior and design features of steel structures. Salim and Davalos [6] expanded the Vlasov's theory to perform the linear analysis of open- and closed-section laminated composite beams. The effect of warping torsion is also considered, and a close agreement among analytical, experimental, and finite element results is reported. Shin and Kim [7] obtained an exact solution for twist angle and fiber stresses of TWBs made of composite materials with single- and double-celled sections subjected to a torsional moment. Liu et al. [8] studied the axial–torsional vibration of pre-twisted beams and obtained a set of criteria for checking the validity of the simplifying assumptions used in the prismatic beam warping function. Pi and Trahair [9] presented a finite element solution of the nonlinear torsional analysis of I-section beams considering large twist rotations. They concluded that I-section beams have much larger torsional capacities than can be predicted by linear plastic collapse analysis. Trahair [10] investigated the nonlinear twisting rotation of a TWB with open section that includes the effects of nonlinear Wagner stiffening torques. Then he extended the nonlinear analysis to members of more general cross-sections and solved the nonlinear equations with the finite element method. To show the importance of the problem of nonlinear angle of twist, he stated that although nonlinear effects rarely occur in practice because of serviceability considerations, some aspects of member strength may be influenced by nonlinear torsion effects for a number of reasons. First, the strengthening effects of nonlinear torsion allow torsion members to become fully plastic. Therefore, the use of plastic methods of strength design for torsion is applicable [5]. Second, the nonlinear torsional effects made the post-lateral buckling of beams imperfection insensitive. Third, the stiffening effects of the nonlinear torsion justify the lateral buckling strength of a beam that is bent about its strong axis and cannot be less than its weak axis in-plane strength. Pi et al. [11] presented a new spatially curved-beam element with warping and Wagner effects that can be used for the nonlinear large displacement analysis of structures. This element is accurate and efficient for the nonlinear elastic, buckling, and post-buckling analysis of arches. A close agreement among analytical, experimental, and numerical results is reported. Mohri et al. [12] investigated a nonlinear model for large torsion analysis of TWBs including shortening effect [13], pre-buckling deflections, and flexural–torsional couplings. This model is extended further to finite element formulation, and then, the corresponding nonlinear equations are solved using the incremental iterative Newton–Raphson method. Sapountzakis and Tsipiras [14] obtained a boundary element solution for the torsional vibration problem of bars of arbitrary doubly symmetric cross-section. Furthermore, they [15] utilized boundary element method in nonlinear torsional analysis of doubly symmetric cross-sectional bars at torsional post-buckling configuration in both free vibration and primary resonance cases. They have shown that in the case of primary resonance excitation of a bar in torsion at a pre-buckled state, the response could consist of a beating phenomenon. However, there are many other studies that used analytical or numerical solutions, devoted to the linear and nonlinear torsional behavior of beams [16–27]. They come to the conclusion that shortening effect plays an important role in torsional vibrations, and also, that the validity of Vlasov's theory is poor in comparison with the experimental results.

Although there exist a large number of research works on the nonlinear torsional vibrations of TWBs, to the best of the authors' knowledge, there has been no study about nonlinear normal modes and internal resonance in the nonlinear torsional vibrations of TWBs including shortening effect. The aim of this study is to

(i) present a perturbation solution for nonlinear torsional vibrations of a straight isotropic TWB,
(ii) parametrically represent the nonlinear torsional dynamic of the TWB in different boundary conditions,
(iii) study the vibration frequency-amplitude dependence of the TWB in torsion,
(iv) study the occurrence of internal resonance in the nonlinear torsional vibrations of the TWB whenever the torsional frequencies are commensurable or near commensurable,
(v) investigate the effect of the warping on the torsional mode's coupling of the TWB
(vi) identify the nonlinear normal modes of the TWB in torsion
(vii) study the stability of the nonlinear normal modes of the TWB in torsion.

The structural model considered here incorporates a number of nonclassical effects including primary and secondary warpings, warping inertia, nonuniform torsional model, and rotary inertia. The TWB is assumed to be adequately laterally supported so that it does not exhibit any flexural or flexural–torsional behavior. The free vibration problem is solved using the Galerkin discretization and the method of multiple scales. The obtained results are compared with the available results in the literature that are obtained from boundary element and finite element methods, which reveals an excellent agreement between different solution methodologies.

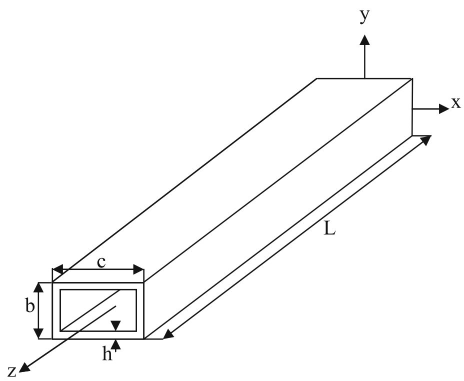

Fig. 1 Schematic description of the TWB and its cross-section

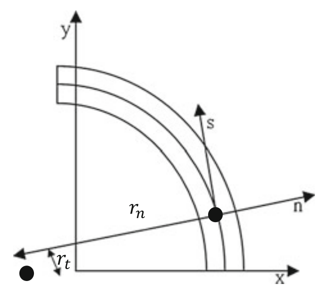

Fig. 2 Cross-sectional coordinates to define complex cross-sections

2 The equations of motion

The structural model consists of a straight uniform box beam with the length of L, width of c, height of b, and thickness of h (Fig. 1). The reference coordinates (x, y, z) are defined as local coordinates associated with the beam, and another set of coordinates (s, n, z) is used to define the cross-sectional profile (Fig. 2). The z-axis is located as to coincide with the locus of the symmetric point of the box beam cross-section along the beam span.

In order to get pertinent kinematic results to be used later, only the expressions related to the twisting rotation and extension will be retained. The position of a point of the beam cross-section after deformation, subscript 'd', can be stated as

$$\begin{aligned} x_d &= x\cos\phi - y\sin\phi, \\ y_d &= x\sin\phi + y\cos\phi, \\ z_d &= z + w_0 - \phi'(z,t)(F_w(s) - nr_t(s)), \end{aligned} \tag{1}$$

where ϕ and w_0 denote the angle of twist and average axial deformation [14] of the TWB, respectively. Also, a prime denotes the derivative with respect to the z-coordinate. The primary warping function (F_w) for the box beam can be written as

$$F_w = \int_0^s [r_n(\bar{s}) - \Psi]\mathrm{d}\bar{s}. \tag{2}$$

The perpendicular distances from shear center of the cross-section to the tangent and normal lines of the mid-line beam contour, $r_n(s)$ and $r_t(s)$, respectively (Fig. 2), are defined as

$$\begin{aligned} r_t(s) &= x(s)\frac{\mathrm{d}x}{\mathrm{d}s} + y(s)\frac{\mathrm{d}y}{\mathrm{d}s}, \\ r_n(s) &= -y(s)\frac{\mathrm{d}x}{\mathrm{d}s} + x(s)\frac{\mathrm{d}y}{\mathrm{d}s}. \end{aligned} \tag{3}$$

Also, the torsional function Ψ is defined as

$$\Psi = \frac{\oint r_n(s)\mathrm{d}s}{\oint \mathrm{d}s}. \tag{4}$$

Hence, the displacement field can be obtained as

$$\begin{aligned} u(x, y, z, t) &= x_d - x = x(\cos\phi - 1) - y\sin\phi, \\ v(x, y, z, t) &= y_d - y = x\sin\phi + y(\cos\phi - 1), \\ w(x, y, z, t) &= w_0 - \phi'(z, t)(\underline{F_w(s)} - \underline{\underline{nr_t(s)}}). \end{aligned} \tag{5}$$

In Eq. (4), the terms associated with primary and secondary warping are underscored by one and two superposed solid lines (see Ref. [28]). The components of acceleration vector can be written as

$$\begin{aligned} a_x &= -\ddot{\phi}(x\sin\phi + y\cos\phi) - \dot{\phi}^2(x\cos\phi - y\sin\phi), \\ a_y &= -\ddot{\phi}(y\sin\phi - x\cos\phi) - \dot{\phi}^2(x\sin\phi + y\cos\phi). \\ a_z &= \ddot{w}_0 - \ddot{\phi}'(F_w(s) - nr_t(s)). \end{aligned} \tag{6}$$

The axial strain is defined as

$$\varepsilon_{zz} = \frac{\mathrm{d}S - \mathrm{d}s}{\mathrm{d}s}, \tag{7}$$

where

$$\begin{aligned} \left(\frac{\mathrm{d}S}{\mathrm{d}z}\right)^2 &= x_d'^2 + y_d'^2 + z_d'^2 \\ &= 1 + 2\left(w_0' - \phi''(z, t)(F_w(s) - nr_t(s))\right) + \phi'^2(x^2 + y^2). \end{aligned} \tag{8}$$

$\mathrm{d}s/\mathrm{d}z$ obtained in similar manner in absence of elastic deformations. Hence, the strain field is obtained as

$$\begin{aligned} \varepsilon_{zz}(n, s, z, t) &= \varepsilon_{zz}^0(s, z, t) + n\varepsilon_{zz}^n(s, z, t), \\ \varepsilon_{zz}^0(s, z, t) &= w_0' - \phi''(z, t)F_w(s) + \underline{\frac{1}{2}\phi'^2(x^2 + y^2)}, \\ \varepsilon_{zz}^n(s, z, t) &= r_t(s)\phi''(z, t), \\ \gamma_{sz}(s, z, t) &= \psi(s, z)\phi'(z). \end{aligned} \tag{9}$$

The term above the solid line in the longitudinal strain is a nonlinear term, absent in Vlasov's model called Wagner strain [13].

Constitutive relations for an isotropic material can be written as

$$\begin{Bmatrix} \sigma_{ss} \\ \sigma_{zz} \\ \sigma_{zn} \\ \sigma_{sn} \\ \sigma_{sz} \end{Bmatrix} = \begin{bmatrix} Q_{11} & Q_{12} & 0 & 0 & 0 \\ Q_{12} & Q_{22} & 0 & 0 & 0 \\ 0 & 0 & Q_{44} & 0 & 0 \\ 0 & 0 & 0 & Q_{44} & 0 \\ 0 & 0 & 0 & 0 & Q_{66} \end{bmatrix} \begin{Bmatrix} \varepsilon_{ss} \\ \varepsilon_{zz} \\ \gamma_{zn} \\ \gamma_{sn} \\ \gamma_{sz} \end{Bmatrix}, \tag{10}$$

where

$$Q_{11} = Q_{22} = \frac{E}{1 - \nu^2}, \quad Q_{12} = \frac{E\nu}{1 - \nu^2}, \quad Q_{44} = Q_{55} = k^2G, \quad Q_{66} = \frac{E}{2(1 + \nu)}. \tag{11}$$

E, ν, k are Young's modulus of elasticity, Poisson's ratio, and the shear correction factor. The stress resultants N_{zz}, N_{sz} and the stress couple L_{zz} are defined as

$$(N_{zz}, L_{zz}) = \int_{-\frac{h}{2}}^{\frac{h}{2}} \sigma_{zz}(1, n)\mathrm{d}n, \tag{12}$$

$$N_{sz} = \int_{-\frac{h}{2}}^{\frac{h}{2}} \sigma_{sz}\mathrm{d}n. \tag{13}$$

Substituting Eq. (10) into Eqs. (12) and (13) and assuming the hoop stress to be negligible, then the 2-D stress resultants and stress couples are obtained as

$$\begin{Bmatrix} N_{zz} \\ N_{sz} \\ L_{zz} \end{Bmatrix} = \begin{bmatrix} k_{11} & 0 & k_{14} \\ 0 & k_{23} & 0 \\ k_{14} & 0 & k_{44} \end{bmatrix} \begin{Bmatrix} \varepsilon_{zz}^{0} \\ \phi' \\ \varepsilon_{zz}^{n} \end{Bmatrix}, \tag{14}$$

where the k_{ij} are defined as

$$\begin{aligned} k_{11} &= A_{22} - \frac{A_{12}^{2}}{A_{11}}, \qquad & k_{14} &= B_{22} - \frac{A_{12}B_{12}}{A_{11}}, \\ k_{22} &= A_{66}, & k_{23} &= 2k_{22}\Psi, \\ k_{44} &= D_{22} - \frac{B_{12}^{2}}{A_{11}}. \end{aligned} \tag{15}$$

The stiffness quantities A_{ij} and B_{ij} are defined as

$$A_{ij}, B_{ij} = \int_{-\frac{h}{2}}^{\frac{h}{2}} Q_{ij}(1, n)\mathrm{d}n. \tag{16}$$

The one-dimensional stress measures T_r, M_p, B_w can be defined in terms of stress resultants and stress couples:

$$T_z(z, t) = \oint N_{zz}\,\mathrm{d}s, \tag{17}$$

$$T_r(z, t) = \oint N_{zz}(x^2 + y^2)\,\mathrm{d}s, \tag{18}$$

$$M_z(z, t) = \oint N_{sz}\Psi\mathrm{d}s, \tag{19}$$

$$B_w(z, t) = \oint (F_w N_{zz} - r_t L_{zz})\,\mathrm{d}s. \tag{20}$$

Substituting Eq. (9) into Eqs. (12), (17) and (18), and considering the integral of warping function and ignoring the effects of the secondary warping, T_z and T_r are obtained as

$$T_z = k_{11}S\left(w_0' + \frac{1}{2}\frac{\widehat{I}_p}{S}\phi'^2\right), \tag{21}$$

$$T_r = \frac{T_z\widehat{I}_p}{S} + \frac{1}{2}B\phi'^2, \tag{22}$$

where

$$S = \oint \mathrm{d}s, \tag{23}$$

$$B = k_{11}\left(I_{ps} - \frac{\widehat{I}_p^{\,2}}{S}\right), \tag{24}$$

$$\widehat{I}_p = \oint \left(x^2 + y^2\right) \mathrm{d}s, \tag{25}$$

$$I_{ps} = \oint \left(x^2 + y^2\right)^2 \mathrm{d}s. \tag{26}$$

Also, M_z and B_w can be written in terms of the displacement field as

$$M_z = a_{77}\phi', \tag{27}$$

$$B_w = -a_{66}\phi'', \tag{28}$$

where

$$a_{77} = \oint \Psi k_{23} \mathrm{d}s, \tag{29}$$

$$a_{66} = \oint \left(F_w^2 k_{11} + 2F_w r_t k_{14} + r_t^2 k_{44}\right) \mathrm{d}s. \tag{30}$$

The reduced mass terms are defined as

$$m = \oint \int_{-\frac{h}{2}}^{\frac{h}{2}} \rho \, \mathrm{d}n \, \mathrm{d}s, \tag{31}$$

$$I_p = \oint \int_{-\frac{h}{2}}^{\frac{h}{2}} \rho (x^2 + y^2) \, \mathrm{d}n \, \mathrm{d}s, \tag{32}$$

$$\bar{I}_p = \oint \int_{-\frac{h}{2}}^{\frac{h}{2}} \rho (x^2 - y^2) \, \mathrm{d}n \, \mathrm{d}s, \tag{33}$$

$$I_{ww} = \oint \int_{-\frac{h}{2}}^{\frac{h}{2}} \rho \left(F_w^2 + n^2 r_t^2\right) \, \mathrm{d}n \, \mathrm{d}s. \tag{34}$$

The governing differential equations of motion are derived using Hamilton's principle in the absence of body forces and surface shear forces. Hamilton's principle is expressed as follows:

$$\int_{t_1}^{t_2} (\delta U + \delta W - \delta T) \mathrm{d}t = 0, \tag{35}$$

where U, T, and W are the potential energy, kinetic energy, and work done by external force of the system, respectively, and t_1 and t_2 are two arbitrary points in time. The energy variations can be written as

$$\delta U = \frac{1}{2}\oint \int_0^L \left(N_{zz}\delta\varepsilon_{zz}^0 + L_{zz}\delta\varepsilon_{zz}^1 + N_{sz}\delta\gamma_{sz}\right)\mathrm{d}s\,\mathrm{d}z, \tag{36}$$

$$\delta T = \oint \int_0^L \rho\left(a_x\delta u + a_y\delta v + a_z\delta w\right)\mathrm{d}s\,\mathrm{d}z. \tag{37}$$

Substituting Eqs. (6), (9), (17)–(20) and (31)–(34) into Eqs. (36) and (37) yields

$$\int_{t_1}^{t_2}\delta U\,\mathrm{d}t = \int_{t_1}^{t_2}\left\{\int_0^L -\left[T_z'\delta w_0 + \left(B_w + \left(T_r\phi'\right)' + M_z'\right)\right]\delta\phi\,\mathrm{d}z \right.$$
$$\left. + \left[T_z\delta w_0 - B_w\delta\phi' + \left(B_w' + T_r\phi' + M_z\right)\delta\phi\right]\Big|_0^L\right\}\mathrm{d}t, \tag{38}$$

$$\int_{t_1}^{t_2}\delta T\,\mathrm{d}t = -\int_{t_1}^{t_2}\left\{\int_0^L b_1\ddot{w}_0\delta w_0 + \left(I_p\ddot{\phi} - \left(I_{ww}\ddot{\phi}'\right)'\right)\delta\phi\mathrm{d}z + I_{ww}\ddot{\phi}'\delta\phi\Big|_0^L\right\}\mathrm{d}t. \tag{39}$$

In the case of free vibration, the Euler–Lagrange equation of motion for large twist angle can be obtained from Eqs. (35), (38) and (39) as

$$\delta w : T_z' - b_1\ddot{w}_0 = 0, \tag{40}$$
$$\delta\phi : B_w'' + \left(T_r\phi'\right)' + M_z' - I_p\ddot{\phi} + \left(I_{ww}\ddot{\phi}'\right)' = 0. \tag{41}$$

The boundary conditions (B.C.) at two edges of the beam can be stated as

$$\begin{aligned} \delta w_0 = 0 \quad &\text{or} \quad T_z = 0,\\ \delta\phi = 0 \quad &\text{or} \quad B_w' + M_z + T_r\phi' + I_{ww}\ddot{\phi}' = 0,\\ \delta\phi' = 0 \quad &\text{or} \quad B_w = 0. \end{aligned} \tag{42}$$

Hence, using Eqs. (21)–(34), one can write the Navier form of governing differential equations of motion in terms of unknown displacement functions as

$$\delta w : k_{11}Sw_0'' + k_{11}\bar{I}_p\phi'\phi'' - b_1\ddot{w}_0 = 0, \tag{43}$$
$$\delta\phi : -\left(a_{66}\phi''\right)'' + \left(k_{11}\bar{I}_p w_0'\phi' + \frac{1}{2}\bar{B}\phi'^3\right)' + \left(a_{77}\phi'\right)' - I_p\ddot{\phi} + \left(I_{ww}\ddot{\phi}'\right)' = 0, \tag{44}$$

where $\bar{B} = k_{11}I_{ps}$. In Eq. (44), the first term is associated with the restrained warping. a_{77} presents the usual Saint-Venant torsional rigidity of the beam. and the term including $\bar{B}$ is the nonlinear term due to the shortening effect. It should be remarked that Eqs. (43) and (44) coincide with those obtained by Sapountzakis and Tsipiras [14] for the beam with solid cross-section.

In order to reduce the governing equations to a single equation, axial inertia should be neglected, and subsequently, w_0 could be exactly eliminated in Eqs. (43) and (44) [14]. Hence,

$$w_0'' = -\frac{\bar{I}_p}{S}\phi'\phi'', \tag{45}$$

which after integration leads to,

$$w_0' = -\frac{1}{2}\frac{\bar{I}_p}{S}\phi'^2 + \frac{\bar{T}_z}{k_{11}S}. \tag{46}$$

In the case of constant axial load acting along the bar, $\bar{T}_z$ is equal to this axial load, while for a TWB with axially immovable ends, $\bar{T}_z$ represents axial load induced by geometrical nonlinearity,

$$\bar{T}_z = \frac{1}{2}\frac{k_{11}\bar{I}_p}{L}\int_0^L \phi'^2 \mathrm{d}z. \tag{47}$$

Substituting Eq. (46) into Eq. (44) leads to

$$\delta\phi : \left(a_{66}\phi''\right)'' - \left(\frac{\bar{I}_p}{S}\bar{T}_z\phi' + \frac{1}{2}B\phi'^3\right)' - \left(a_{77}\phi'\right)' + I_p\ddot{\phi} - \left(I_{ww}\ddot{\phi}'\right)' = 0. \tag{48}$$

Static counterpart of Eq. (48) obtained by neglecting all inertia terms coincides with those obtained by Trahair [10] for an isotropic thin-walled beam.

3 Discretized equation of motion and perturbation solution

The Galerkin discretization technique is used to obtain a reduced-order model of the beam. In this regard, the system response is assumed to be in the form

$$\phi(z,t) = \sum_{i=1}^{N}\hat{\phi}_i(z)q_i(t), \tag{49}$$

where N, $\hat{\phi}_i(z)$, and $q_i(t)$ are a finite integer, the characteristic torsional modes of the beam with associated boundary conditions, and the generalized coordinates, respectively. The Galerkin method can be used to transfer the partial differential equation of motion into a set of ordinary differential equations. Application of the perturbation methods to the reduced-order model of a nonlinear continuous system with quadratic nonlinearities may lead to both quantitative and qualitative errors [29]. It should be noted that such a problem does not occur in the system represented by Eq. (48) containing only cubic nonlinearities. Here, nonlinear torsional vibrations of TWBs with clamped–clamped and clamped-free torsional boundary conditions are investigated using the two-mode Galerkin's method.

3.1 Torsionally clamped–clamped TWB

The linear torsional mode shapes of the clamped–clamped TWB are

$$\hat{\phi}_i(z) = \sin\left(\frac{\mathrm{i}\pi z}{L}\right). \tag{50}$$

Substituting Eqs. (49) and (50) into Eq. (48) in the presence of external axial loading, taking the inner product of the equation with the corresponding mode shape, and using the orthogonality properties of the mode shapes, the following discretized equations of motion are obtained:

$$\begin{aligned}\ddot{q}_1 + \omega_1^2 q_1 &= \gamma_1 q_1^3 + \gamma_2 q_1 q_2^2,\\ \ddot{q}_2 + \omega_2^2 q_2 &= \gamma_3 q_1^2 q_2 + \gamma_4 q_2^3,\end{aligned} \tag{51}$$

where

$$\begin{aligned}
\omega_1^2 &= \frac{\pi^2L^2\left(\frac{\bar{I}_p}{S}\bar{T}_z + a_{77}\right) + \pi^4 a_{66}}{L^4 I_p + \pi^2 L^2 I_{ww}}, & \omega_2^2 &= \frac{4\pi^2L^2\left(\frac{\bar{I}_p}{S}\bar{T}_z + a_{77}\right) + 16\pi^4 a_{66}}{L^4 I_p + 4\pi^2 L^2 I_{ww}},\\
\gamma_1 &= \frac{-3}{8}\frac{B\pi^4}{L^4 I_p + \pi^2 L^2 I_{ww}}, & \gamma_2 &= \frac{-3B\pi^4}{L^4 I_p + \pi^2 L^2 I_{ww}},\\
\gamma_3 &= \frac{-3B\pi^4}{L^4 I_p + 4\pi^2 L^2 I_{ww}}, & \gamma_4 &= \frac{-6B\pi^4}{L^4 I_p + 4\pi^2 L^2 I_{ww}}.
\end{aligned} \tag{52}$$

In the case of a free warping ($a_{66} = I_{ww} = 0$) TWB without axial loading,

$$\omega_1 = \frac{\pi}{L}\sqrt{\frac{a_{77}}{I_p}}, \quad \omega_2 = \frac{2\pi}{L}\sqrt{\frac{a_{77}}{I_p}}. \tag{53}$$

It should be mentioned that in this case, the two-to-one internal resonance between first and second modes is not available because the nonlinear interaction terms are equal to zero [30]. The method of multiple scales is used to obtain the modulation equations governing the amplitude and phase of the torsional modes. The new independent variables are defined as

$$T_n = \varepsilon^n t, \quad n = 0, 1, 2, \ldots \tag{54}$$

Therefore, the derivatives with respect to time are replaced by the partial derivatives with respect to the new variables. That is,

$$\begin{aligned} \frac{\mathrm{d}}{\mathrm{d}t} &= \frac{\mathrm{d}T_0}{\mathrm{d}t}\frac{\partial}{\partial T_0} + \frac{\mathrm{d}T_1}{\mathrm{d}t}\frac{\partial}{\partial T_1} + \cdots = D_0 + \varepsilon D_1 + \cdots, \\ \frac{\mathrm{d}^2}{\mathrm{d}t^2} &= D_0^2 + 2\varepsilon D_0 D_1 + \varepsilon^2(D_1^2 + 2D_0D_2) + \cdots. \end{aligned} \tag{55}$$

The solution of Eq. (51) can be stated as

$$\begin{aligned} q_1(t,\varepsilon) &= \varepsilon q_{11}(T_0, T_2) + \varepsilon^3 q_{13}(T_0, T_2) + O\left(\varepsilon^4\right), \\ q_2(t,\varepsilon) &= \varepsilon q_{21}(T_0, T_2) + \varepsilon^3 q_{23}(T_0, T_2) + O\left(\varepsilon^4\right). \end{aligned} \tag{56}$$

Substituting Eqs. (55) and (56) in Eq. (51) and equating the coefficients of the ε-terms of same power yields the following system of equations:

$$\begin{aligned} D_0^2 q_{11} + \omega_1^2 q_{11} &= 0, \\ D_0^2 q_{21} + \omega_2^2 q_{21} &= 0, \end{aligned} \tag{57}$$

$$\begin{aligned} D_0^2 q_{13} + \omega_1^2 q_{13} &= -2D_0D_2q_{11} + \gamma_1 q_{11}^3 + \gamma_2 q_{11} q_{21}^2, \\ D_0^2 q_{23} + \omega_2^2 q_{23} &= -2D_0D_2q_{21} + \gamma_3 q_{11}^2 q_{21} + \gamma_4 q_{21}^3, \end{aligned} \tag{58}$$

where ω_i is the linear natural frequency of Eq. (51). The general solution of Eq. (57) can be written as

$$\begin{aligned} q_{11} &= A_1(T_2)\,\mathrm{e}^{\mathrm{i}\omega_1 T_0} + \text{c.c.}, \\ q_{21} &= A_2(T_2)\,\mathrm{e}^{\mathrm{i}\omega_2 T_0} + \text{c.c.}, \end{aligned} \tag{59}$$

where c.c. denotes the complex conjugate of the complex expressions. Substituting the general solutions of Eq. (57) into Eq. (58) yields

$$\begin{aligned} D_0^2 q_{13} + \omega_1^2 q_{13} &= \left(-2\mathrm{i}\omega_1 A_1^* + 3\gamma_1 A_1^2\bar{A}_1 + 2\gamma_2 A_2\bar{A}_2 A_1\right)\mathrm{e}^{\mathrm{i}\omega_1 T_0} + \gamma_1 A_1^3 \mathrm{e}^{3\mathrm{i}\omega_1 T_0} \\ &\quad + \gamma_2 A_1 A_2^2 \mathrm{e}^{\mathrm{i}(\omega_1+2\omega_2)T_0} + \gamma_2 A_1 \bar{A}_2^2 \mathrm{e}^{\mathrm{i}(\omega_1-2\omega_2)T_0} + \text{c.c.}, \\ D_0^2 q_{23} + \omega_2^2 q_{23} &= \left(-2\mathrm{i}\omega_2 A_2^* + 3\gamma_4 A_2^2\bar{A}_2 + 2\gamma_3 A_1\bar{A}_1 A_2\right)\mathrm{e}^{\mathrm{i}\omega_2 T_0} + \gamma_4 A_2^3 \mathrm{e}^{3\mathrm{i}\omega_2 T_0} \\ &\quad + \gamma_3 A_1^2 A_2 \mathrm{e}^{\mathrm{i}(2\omega_1+\omega_2)T_0} + \gamma_4 \bar{A}_1^2 A_2 \mathrm{e}^{\mathrm{i}(\omega_2-2\omega_1)T_0} + \text{c.c.}, \end{aligned} \tag{60}$$

where a superscript $*$ denotes the differentiation with respect to T_2 and $\bar{A}_m$ is the complex conjugate of A_m. Secular terms will be eliminated from Eq. (60) if A_m is the solution of

$$\begin{aligned} &-2\mathrm{i}\omega_1 A_1^* + 3\gamma_1 A_1^2\bar{A}_1 + 2\gamma_3 A_2\bar{A}_2 A_1 = 0, \\ &-2\mathrm{i}\omega_2 A_2^* + 3\gamma_4 A_2^2\bar{A}_2 + 2\gamma_3 A_1\bar{A}_1 A_2 = 0. \end{aligned} \tag{61}$$

Table 1 Fundamental torsional frequency ω_1 and induced axial load $\bar{T}_z$ of a TWB with clamped–clamped torsional boundary conditions and immovable ends

		Present study		Ref. [14]		Ref. [21]
		$B \neq 0$	$B = 0$	$B \neq 0$	$B = 0$	$B = 0$
$\omega_1 (s^{-1})$						
Linear		214.22	214.22	214.23	214.23	207.23
$\phi(L/2)$ (rad)	0.1	214.96	214.76	215.04	214.78	207.83
	0.2	217.16	216.38	217.44	216.40	209.62
	1.5	343.94	313.76	348.86	313.77	–
$\bar{T}_z (kN)$						
Linear		–	–	–	–	–
$\phi(L/2)$ (rad)	0.1	17.6	17.6	17.60	17.60	19.43
	0.2	70.39	70.39	70.36	70.39	77.72
	1.5	3,959.50	3,959.50	3,891.26	3,959.63	–

$a_{77} = 16,848\,\text{Nm}^2$, $a_{66} = 25,200\,\text{Nm}^4$, $B = 34{,}251\,\text{Nm}^4$, $I_p = 0.434\,\text{kgm}$, $I_{ww} = 9.6 \times 10^{-4}\text{kgm}^3$

Assuming $A_m = \frac{1}{2} a_m \exp(\mathrm{i}\theta_m)$, substituting in Eq. (61) and separating real and imaginary parts leads to

$$a_1^* = 0, \tag{62}$$

$$a_2^* = 0, \tag{63}$$

$$\theta_1^* = -\left(\frac{3\gamma_1}{8\omega_1} a_1^2 + \frac{\gamma_2}{4\omega_1} a_2^2\right), \tag{64}$$

$$\theta_2^* = -\left(\frac{3\gamma_4}{8\omega_2} a_2^2 + \frac{\gamma_3}{4\omega_2} a_1^2\right). \tag{65}$$

Therefore,

$$a_1 = a_{10}, \tag{66}$$

$$a_2 = a_{20}, \tag{67}$$

$$\theta_1 = -\left(\frac{3\gamma_1}{8\omega_1} a_{10}^2 + \frac{\gamma_2}{4\omega_1} a_{20}^2\right) \varepsilon^2 t + \theta_{10}, \tag{68}$$

$$\theta_2 = -\left(\frac{3\gamma_4}{8\omega_2} a_{20}^2 + \frac{\gamma_3}{4\omega_2} a_{10}^2\right) \varepsilon^2 t + \theta_{20}, \tag{69}$$

where a_{10}, a_{20}, θ_{10}, and θ_{20} are constants of integration. It should be noted that phases and hence the nonlinear frequencies are functions of the amplitudes.

For validation, the fundamental nonlinear natural frequency and induced axial load ($\bar{T}_z$) of an axially immovable TWB obtained in the context of this study are compared with those obtained by Sapountzakis and Tsipiras [14] and Rozmarynowski and Szymczak [21] using boundary element and finite element methods, respectively. Table 1 shows an excellent agreement between the results of this study and those obtained via boundary element and finite element methods. Since the assumed mode shapes (Eq. (50)) are not altered by the axial load ($\bar{T}_z$) or the geometric cross-sectional constant B, the obtained induced axial loads ($\bar{T}_z$) are the same values in the presence or absence of the parameter B (Eq. (47)).

3.2 Torsionally clamped-free TWB

The linear mode shapes of a torsionally clamped-free TWB are

$$\hat{\phi}_i(z) = \sin\left(\frac{(2\mathrm{i}-1)\,\pi z}{2L}\right). \tag{70}$$

Substituting Eqs. (49) and (70) into Eq. (48) leads to the following discretized equation of motion:

$$\begin{aligned} \ddot{q}_1 + \omega_1^2 q_1 &= \gamma_1 q_1^3 + \gamma_2 q_1^2 q_2 + \gamma_3 q_1 q_2^2, \\ \ddot{q}_2 + \omega_2^2 q_2 &= \gamma_4 q_1^3 + \gamma_5 q_1^2 q_2 + \gamma_6 q_2^3, \end{aligned} \tag{71}$$

where

$$\omega_1^2=\frac{4\pi^2L^2\left(\frac{\bar{I}_p}{S}\bar{T}_z+a_{77}\right)+\pi^4a_{66}}{16L^4I_p+4\pi^2L^2I_{ww}},\quad \omega_2^2=\frac{288\pi^2L^2\left(\frac{\bar{I}_p}{S}\bar{T}_z+a_{77}\right)+648\pi^4a_{66}}{128L^4I_p+288\pi^2L^2I_{ww}},$$
$$\gamma_1=\frac{-3B\pi^4}{128L^4I_p+32\pi^2L^2I_{ww}},\quad \gamma_2=\frac{-9B\pi^4}{128L^4I_p+32\pi^2L^2I_{ww}},$$
$$\gamma_3=\frac{-54B\pi^4}{128L^4I_p+32\pi^2L^2I_{ww}},\quad \gamma_4=\frac{-3B\pi^4}{128L^4I_p+288\pi^2L^2I_{ww}},$$
$$\gamma_5=\frac{-54B\pi^4}{128L^4I_p+288\pi^2L^2I_{ww}},\quad \gamma_6=\frac{-243B\pi^4}{128L^4I_p+288\pi^2L^2I_{ww}}. \tag{72}$$

In the case of a free warping ($a_{66}=I_{ww}=0$) TWB without axial loading,

$$\omega_1=\frac{\pi}{2L}\sqrt{\frac{a_{77}}{I_p}},\quad \omega_2=\frac{3\pi}{2L}\sqrt{\frac{a_{77}}{I_p}}. \tag{73}$$

The relationship between frequencies ($\omega_2=3\omega_1$) can cause two modes to be coupled, and an internal resonance can exist. Applying the method of multiple scales leads to the following system of equations:

$$D_0^2q_{11}+\omega_1^2q_{11}=0,$$
$$D_0^2q_{21}+\omega_2^2q_{21}=0, \tag{74}$$

$$D_0^2q_{13}+\omega_1^2q_{13}=-2D_0D_2q_{11}+\gamma_1q_{11}^3+\gamma_2q_{11}^2q_{21}+\gamma_3q_{11}q_{21}^2,$$
$$D_0^2q_{23}+\omega_2^2q_{23}=-2D_0D_2q_{21}+\gamma_4q_{11}^3+\gamma_5q_{11}^2q_{21}+\gamma_6q_{21}^3. \tag{75}$$

The general solution of Eq. (74) is in the form of Eq. (59). Hence, one can rewrite Eq. (75) as

$$\begin{aligned}D_0^2q_{13}+\omega_1^2q_{13}&=\left(-2\mathrm{i}\omega_1A_1^*+3\gamma_1A_1^2\bar{A}_1+2\gamma_3A_2\bar{A}_2A_1\right)\mathrm{e}^{\mathrm{i}\omega_1T_0}+2\gamma_2A_1\bar{A}_1A_2\mathrm{e}^{\mathrm{i}\omega_2T_0}\\&\quad+\gamma_1A_1^3\mathrm{e}^{3\mathrm{i}\omega_1T_0}+\gamma_2A_1^2A_2\mathrm{e}^{\mathrm{i}(2\omega_1+\omega_2)T_0}+\gamma_2\bar{A}_1^2A_2\mathrm{e}^{\mathrm{i}(\omega_2-2\omega_1)T_0}\\&\quad+\gamma_3A_1A_2^2\mathrm{e}^{\mathrm{i}(\omega_1+2\omega_2)T_0}+\gamma_3A_1\bar{A}_2^2\mathrm{e}^{\mathrm{i}(\omega_1-2\omega_2)T_0}+\text{c.c.},\\D_0^2q_{23}+\omega_2^2q_{23}&=\left(-2\mathrm{i}\omega_2A_2^*+3\gamma_6A_2^2\bar{A}_2+2\gamma_5A_1\bar{A}_1A_2\right)\mathrm{e}^{\mathrm{i}\omega_2T_0}+3\gamma_4A_1\bar{A}_1A_1\mathrm{e}^{\mathrm{i}\omega_1T_0}\\&\quad+\gamma_4A_1^3\mathrm{e}^{3\mathrm{i}\omega_1T_0}+\gamma_6A_2^3\mathrm{e}^{3\mathrm{i}\omega_2T_0}+\gamma_5A_1^2A_2\mathrm{e}^{\mathrm{i}(2\omega_1+\omega_2)T_0}\\&\quad+\gamma_5\bar{A}_1^2A_2\mathrm{e}^{\mathrm{i}(\omega_2-2\omega_1)T_0}+\text{c.c.}.\end{aligned} \tag{76}$$

As mentioned earlier, without the effects of warping ($a_{66}=I_{ww}=0$) and axial loading $\omega_2=3\omega_1$, but warping and nonlinearity can be treated as detuning parameters which make $\omega_2\approx3\omega_1$ (see Fig. 3), therefore,

$$\omega_2=3\omega_1+\varepsilon^2\sigma,$$
$$\omega_2T_0=3\omega_1T_0+\varepsilon^2\sigma T_0=3\omega_1T_0+\sigma T_2. \tag{77}$$

In Eq. (76), in addition to the terms proportional to $\exp\left(\pm\mathrm{i}\omega_mT_0\right)$, $m=1,2$, secular terms are also produced by the terms proportional to $\exp\left[\pm m\left(\omega_2-2\omega_1\right)T_0\right]$ and $\exp\left(\pm3\mathrm{i}\omega_1T_0\right)$. Secular terms will be eliminated from Eq. (76) if A_m is the solution of

$$-2\mathrm{i}\omega_1A_1^*+3\gamma_1A_1^2\bar{A}_1+2\gamma_3A_2\bar{A}_2A_1+\gamma_2\bar{A}_1^2A_2\mathrm{e}^{\mathrm{i}\sigma T_2}=0,$$
$$-2\mathrm{i}\omega_2A_2^*+3\gamma_6A_2^2\bar{A}_2+2\gamma_5A_1\bar{A}_1A_2+\gamma_4A_1^3\mathrm{e}^{-\mathrm{i}\sigma T_2}=0. \tag{78}$$

Assuming $A_m=\frac{1}{2}a_m\exp(\mathrm{i}\theta_m)$, substituting in Eq. (78), and separating real and imaginary parts leads to

$$8\omega_1a_1^*-\gamma_2a_1^2a_2\sin\lambda=0, \tag{79}$$

$$8\omega_2a_2^*+\gamma_4a_1^3\sin\lambda=0, \tag{80}$$

$$8\omega_1a_1\theta_1^*+\left(3\gamma_1a_1^2+2\gamma_3a_2^2\right)a_1+\gamma_2a_1^2a_2\cos\lambda=0, \tag{81}$$

$$8\omega_2a_2\theta_2^*+\left(3\gamma_6a_2^2+2\gamma_5a_1^2\right)a_2+\gamma_4a_1^3\cos\lambda=0, \tag{82}$$

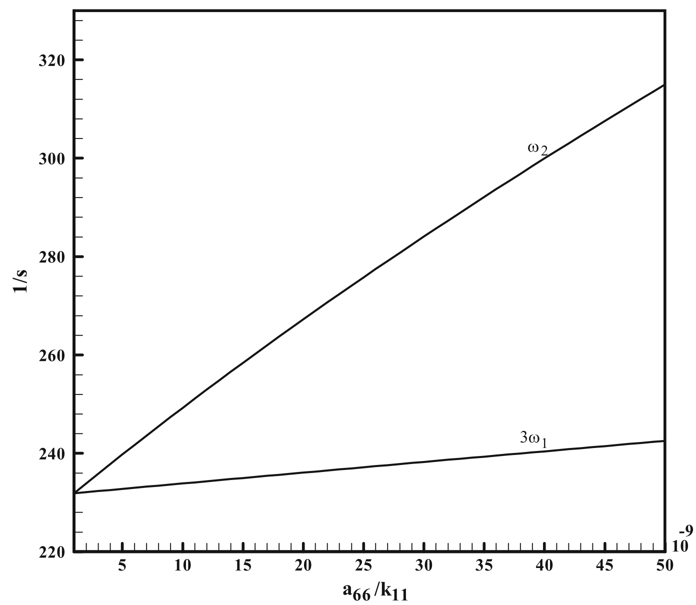

Fig. 3 Variation in $3\omega_1$ and ω_2 of TWB with clamped-free torsional boundary conditions versus a_{66}/k_{11}, $a_{77} = 16,848\,\mathrm{Nm}^2$, $B = 34,251\,\mathrm{Nm}^4$, $I_p = 0.434\,\mathrm{kgm}$, $T_z = 0$

where

$$\lambda = \theta_2 - 3\theta_1 + \sigma T_2. \tag{83}$$

Considering Eqs. (81)–(83), one can write

$$a_2\lambda^* - a_2\sigma - \left(\frac{3\gamma_3}{4\omega_1} - \frac{\gamma_6}{8\omega_2}\right)a_2^3 - \left(\frac{9\gamma_1}{8\omega_1} - \frac{\gamma_5}{4\omega_2}\right)a_1^2a_2 - \left(\frac{3\gamma_2}{8\omega_1}a_1a_2^2 - \frac{\gamma_4}{8\omega_2}a_1^3\right)\cos\lambda = 0. \tag{84}$$

Multiplying Eq. (79) by $\omega_1^{-1}a_1$ and Eq. (80) by $\omega_2^{-1}\nu a_2$, where $\nu = \frac{\gamma_2\omega_2}{\gamma_4\omega_1}$, and adding the results leads to

$$a_1a_1^* + \nu a_2a_2^* = 0. \tag{85}$$

Hence,

$$a_1^2 + \nu a_2^2 = C, \tag{86}$$

where $C$is a constant proportional to the system's initial energy. Now a new variable is ξ, which characterizes the ratio of the first linear mode energy to the total energy, defined as

$$\xi = \frac{a_1^2}{C} = \frac{a_1^2}{a_1^2 + \nu a_2^2}. \tag{87}$$

It must be noted that the $\xi = 0, 1$ correspond to the uncoupled modes, that is, to each linear mode, separately. For the uncoupled modes, the phase difference λ is indefinite, and the frequency response curves for these modes must be obtained from Eqs. (79)–(82).

Stationary or steady-state oscillations are determined by conditions $a_1^* = a_2^* = \lambda^* = 0$. The latter condition means synchronization of the vibrations in two linear modes. From modulation equations (79)–(82), there are two possibilities: $(a_1 = 0, a_2 \neq 0)$ and $(a_1 \neq 0, a_2 \neq 0)$. In the first case, there exists an uncoupled nonlinear normal mode with the frequency (ω_2^{nl}) obtained as

$$\omega_2^{\mathrm{nl}} = \omega_2 + \frac{\mathrm{d}\theta_2}{\mathrm{d}t} = \omega_2 + \varepsilon^2\frac{\mathrm{d}\theta_2}{\mathrm{d}T_2} = \omega_2 - \frac{3\gamma_6\varepsilon^2a_2^2}{8\omega_2}. \tag{88}$$

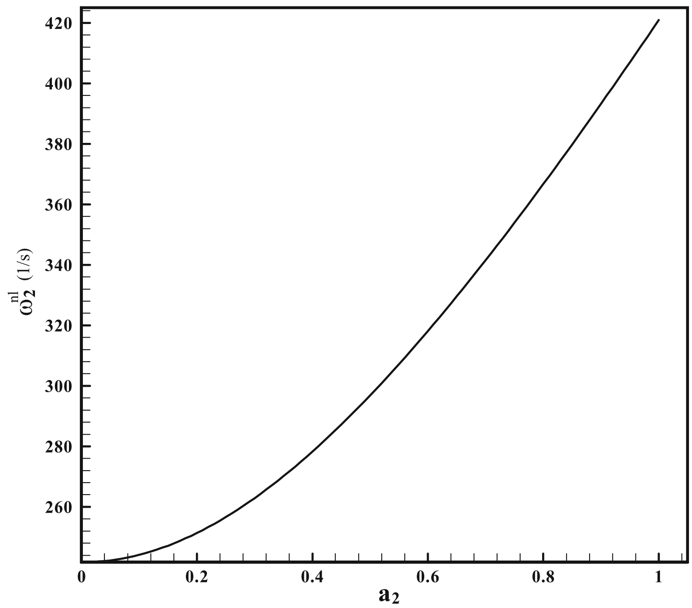

Fig. 4 Variation in the nonlinear frequency of uncoupled naturally stable mode (ω_2^{nl}) of TWB with clamped-free torsional boundary conditions versus its amplitude (a_2) $a_{77} = 16,848\,\mathrm{Nm}^2, a_{66} = 1,050\,\mathrm{Nm}^4, B = 34,251\,\mathrm{Nm}^4, T_z = 0, I_p = 0.434\,\mathrm{kgm}, I_{ww} = 4\times10^{-5}\,\mathrm{kgm}^3, \varepsilon = 0.1, L = 4\,\mathrm{m}$

Figure 4 shows the typical variation in nonlinear natural frequency of the naturally stable uncoupled mode versus its amplitude.

To study the stability of this mode, A_1 and A_2 are assumed to be in the following form:

$$A_1 = \frac{1}{2}(p_1 - q_1)\,\mathrm{e}^{\mathrm{i}sT_2}, \quad A_2 = \frac{1}{2}a_2\mathrm{e}^{\mathrm{i}\theta_2}, \tag{89}$$

where s transforms the resulting equations into an autonomous system. Substituting Eq. (89) into Eq. (78) and separating real and imaginary parts, and linearization of the obtained equations yields

$$\begin{aligned} p_1^* + \left(\frac{1}{3}\left(\sigma + \theta_2^*\right) + \frac{2\gamma_3}{8\omega_1}a_2^2\right) q_1 = 0, \\ q_1^* - \left(\frac{1}{3}\left(\sigma + \theta_2^*\right) + \frac{2\gamma_3}{8\omega_1}a_2^2\right) p_1 = 0. \end{aligned} \tag{90}$$

Therefore, using Eq. (82), the eigenvalues of Eq. (90) are determined in a closed form as

$$\varpi_{1,2} = \pm\mathrm{i}a_2^2\left(\frac{\sigma}{3a_2^2} - \frac{2\gamma_3\omega_2 - \gamma_6\omega_1}{8\omega_1\omega_2}\right). \tag{91}$$

Since the eigenvalues are imaginary values, the uncoupled mode is naturally stable.

In the case of $a_1 \neq 0$, $a_2 \neq 0$, the stationary solutions correspond to

$$\begin{aligned} &\lambda = n\pi, \quad n = 0, 1, 2, \ldots, \\ &\left((-1)^n \frac{\gamma_4}{8}\right)\left(\frac{a_1}{a_2}\right)^3 + \left(\frac{\gamma_5}{4} - \frac{9\omega_2\gamma_1}{8\omega_1}\right)\left(\frac{a_1}{a_2}\right)^2 - \left((-1)^n \frac{3\omega_2\gamma_2}{8\omega_1}\right)\left(\frac{a_1}{a_2}\right) \\ &\quad + \frac{3\gamma_6}{8} - \frac{3\omega_2\gamma_3}{4\omega_1} - \omega_2\frac{\sigma}{a_2^2} = 0, \end{aligned} \tag{92}$$

where $\lambda = n\pi$ corresponds to in-phase and anti-phase oscillations. On the $(a_1 - a_2)$ plane, two normal modes are presented by lines passing through the origin, and extreme values are reached simultaneously. Equation

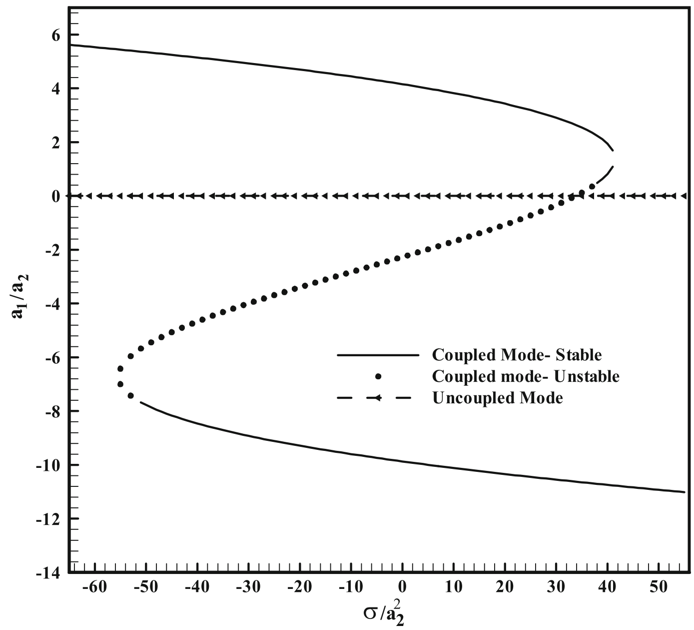

Fig. 5 Variation in the amplitude ratio ($\frac{a_1}{a_2}$) of torsional coupled and uncoupled modes of TWB with clamped-free torsional boundary conditions versus detuning parameter ($\frac{\sigma}{a_2^2}$), $\lambda = 0$, $a_{77} = 16,848\,\mathrm{Nm}^2$, $a_{66} = 1,050\,\mathrm{Nm}^4$, $B = 34,251\,\mathrm{Nm}^4$, $T_z = 0$, $I_p = 0.434\,\mathrm{kgm}$, $I_{ww} = 4 \times 10^{-5}\,\mathrm{kgm}^3$, $L = 4\,\mathrm{m}$

(92) is a cubic equation of $\frac{a_1}{a_2}$, which for a given detuning level has either one or three real roots. The stability of these modes can be determined by studying the stability of the corresponding fixed points of Eqs. (79), (80), and (84) by superposing perturbation parts on the steady-state solutions given by Eq. (92) as

$$\begin{aligned} a_1 &= a_{10} + \varepsilon a_{11}, \\ a_2 &= a_{20} + \varepsilon a_{21}, \\ \lambda &= \lambda_0 + \varepsilon \lambda_1, \end{aligned} \tag{93}$$

where $a_{10}, a_{20}, \lambda_0$ satisfy Eqs. (79), (80) and (84). Substituting Eq. (93) into the modulated equations and expanding for small perturbed parts and keeping linear terms in $a_{11}, a_{21}, \lambda_1$ leads to

$$\begin{aligned} a_{11}^* &= 2\frac{\gamma_2}{8\omega_1} a_{10} a_{20} \sin\lambda_0 a_{11} + \frac{\gamma_2}{8\omega_1} a_{10}^2 \sin\lambda_0 a_{21} + \frac{\gamma_2}{8\omega_1} a_{10}^2 a_{20} \cos\lambda_0 \lambda_1, \\ a_{21}^* &= -3\frac{\gamma_4}{8\omega_2} a_{10}^2 \sin\lambda_0 a_{11} - \frac{\gamma_4}{8\omega_2} a_{10}^3 \cos\lambda_0 \lambda_1, \\ a_{20}\lambda^* &= \left(2\left(\frac{9\gamma_1}{8\omega_1} - \frac{\gamma_5}{4\omega_2}\right) a_{10} a_{20} + \left(\frac{3\gamma_2}{8\omega_1} a_{20}^2 - \frac{3\gamma_4}{8\omega_2} a_{10}^2\right)\cos\lambda_0\right) a_{11} \\ &\quad + \left(\sigma + 3\left(\frac{3\gamma_3}{4\omega_1} - \frac{\gamma_6}{8\omega_2}\right) a_{20}^2 + \left(\frac{9\gamma_1}{8\omega_1} - \frac{\gamma_5}{4\omega_2}\right) a_{10}^2 + \frac{3\gamma_2}{4\omega_1} a_{20} a_{10} \cos\lambda_0\right) a_{21} \\ &\quad - \sin\lambda_0 \left(\frac{3\gamma_2}{8\omega_1} a_{10} a_{20}^2 - \frac{\gamma_4}{8\omega_2} a_{10}^3\right)\lambda_1. \end{aligned} \tag{94}$$

The stability is determined by evaluating the eigenvalues of Eq. (94). The eigenvalues should not have positive real parts to maintain stability. As an example, Fig. 5 shows the variation in the $\frac{a_1}{a_2}$ with $\frac{\sigma}{a_2^2}$. Variation in the detuning parameter leads to either one, two, or three stable coupled modes. Since $\lambda = 0$ and $\lambda = n\pi$, $n = 1, 2, \ldots$ correspond to the same solutions, here only the case of $\lambda = 0$ will be considered. Figure 6, 7, 8 represent the variation in real and imaginary parts of the eigenvalues versus detuning parameter for $\lambda = 0$. There exists one stable coupled mode for $\frac{\sigma}{a_2^2} \leq -55$ and $\frac{\sigma}{a_2^2} \geq 41$, one stable coupled mode and two unstable coupled

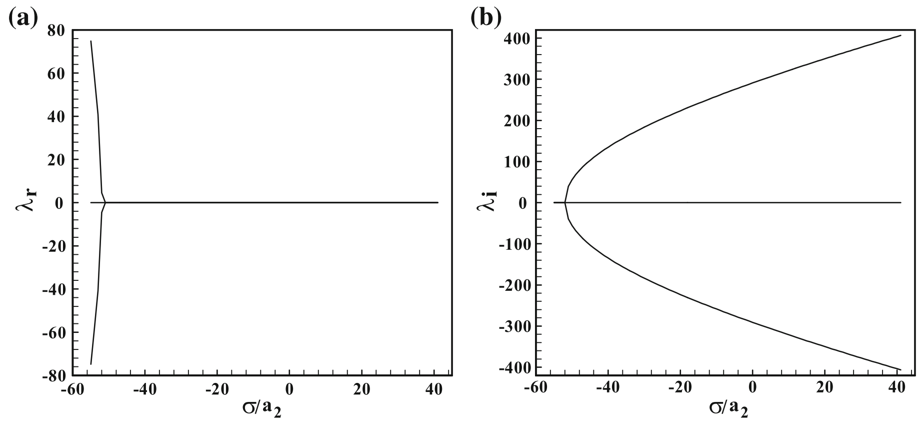

Fig. 6 Variation in the eigenvalues of the first torsional coupled mode of a TWB with clamped-free torsional boundary conditions versus σ/a_2, **a** real part, **b** imaginary part. $\lambda = 0$, $a_{77} = 16,848\,\mathrm{Nm}^2$, $a_{66} = 1,050\,\mathrm{Nm}^4$, $B = 34,251\,\mathrm{Nm}^4$, $T_z = 0$, $I_p = 0.434\,\mathrm{kgm}$, $I_{ww} = 4 \times 10^{-5}\,\mathrm{kgm}^3$, $L = 4\,\mathrm{m}$

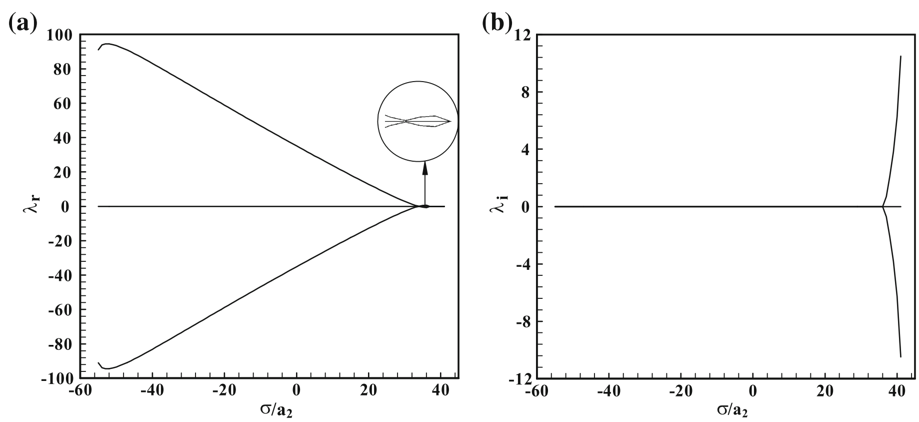

Fig. 7 Variation in the eigenvalues of the second torsional coupled mode of a TWB with clamped-free torsional boundary conditions versus σ/a_2, **a** real part, **b** imaginary part. $\lambda = 0$, $a_{77} = 16,848\,\mathrm{Nm}^2$, $a_{66} = 1,050\,\mathrm{Nm}^4$, $B = 34,251\,\mathrm{Nm}^4$, $T_z = 0$, $I_p = 0.434\,\mathrm{kgm}$, $I_{ww} = 4 \times 10^{-5}\,\mathrm{kgm}^3$, $L = 4\,\mathrm{m}$

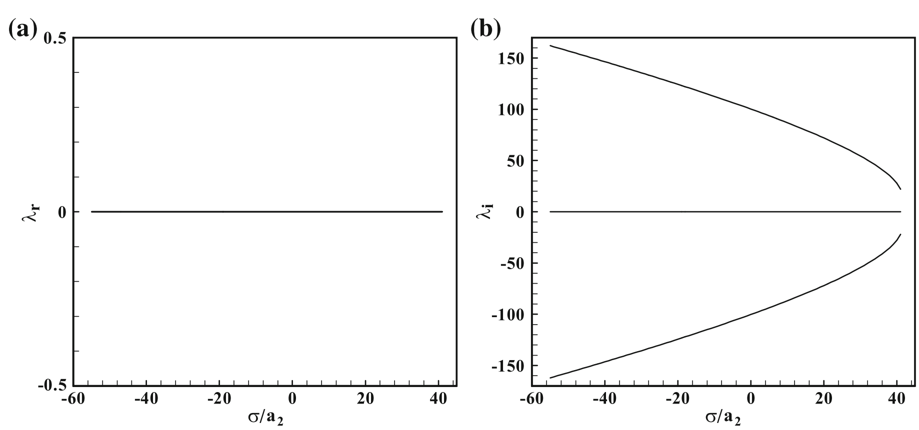

Fig. 8 Variation in the eigenvalues of the third torsional coupled mode of a TWB with clamped-free torsional boundary conditions versus σ/a_2, **a** real part, **b** imaginary part. $\lambda = 0$, $a_{77} = 16,848\,\mathrm{Nm}^2$, $a_{66} = 1,050\,\mathrm{Nm}^4$, $B = 34,251\,\mathrm{Nm}^4$, $T_z = 0$, $I_p = 0.434\,\mathrm{kgm}$, $I_{ww} = 4 \times 10^{-5}\,\mathrm{kgm}^3$, $L = 4\,\mathrm{m}$

modes exist when $40 \le \frac{\sigma}{a_2^2} \le 41$ or $-55 \le \frac{\sigma}{a_2^2} \le -51$, three stable coupled modes exist when $38 \le \frac{\sigma}{a_2^2} \le 40$, and two stable coupled modes and one unstable coupled mode exist for $-51 \le \frac{\sigma}{a_2^2} \le 38$. Figure 5 shows that in a specific level of detuning parameter, the uncoupled stable mode merged with the unstable coupled mode, and the degenerate coupled mode has a multiplicity of two. In the corresponding detuning to amplitude squared ratio, the eigenvalues of the stable coupled mode (Eq. (91)) become zero. Considering both the uncoupled and coupled modes, the system possesses either two or four nonlinear modes.

From another point of view, the first mode, corresponding to the lower branch in Fig. 5, behaves as a center for $\frac{\sigma}{a_2^2} > -55$ and experiences center-saddle bifurcation, when $\frac{\sigma}{a_2^2}$ approaches to -55 from right. The second mode, corresponding to middle branch in Fig. 5, behaves as a saddle point for $-55 \le \frac{\sigma}{a_2^2} \le 38$, as a center for $38 \le \frac{\sigma}{a_2^2} \le 40$ and as an unstable focal point for $40 \le \frac{\sigma}{a_2^2} \le 41$. The third mode, corresponding to the upper branch in Fig. 5, behaves as a center for $\frac{\sigma}{a_2^2} \le 41$, and a center-focal bifurcation occurs at this point.

4 Conclusion

Nonlinear torsional vibrations of a thin-walled beam in the presence of warping effects are investigated. A two-mode Galerkin method is used to discretize the governing differential equation. Then the method of multiple scales is implemented as an approximate method for the time domain solution of the nonlinear equations. Finally, the torsional nonlinear modes of the thin-walled beam in different torsional boundary conditions and their stability are studied. It is shown that in the case of clamped–clamped torsional boundary condition, the phases and the nonlinear frequencies are functions of the amplitudes, and the number of nonlinear normal modes is equal to that of the linear normal modes. In the case of the clamped-free torsional boundary condition, due to the relation between the first two natural frequencies, the cubic nonlinearity in the governing differential equation leads to a three-to-one internal resonance. It is shown that in the case of three-to-one internal resonance between the first and second modes, the beam may possess one stable uncoupled mode and either one stable coupled mode, three stable coupled modes, two stable and one unstable coupled modes, or one stable and two unstable coupled modes.

References

1. Nayfeh, A.H., Mook, D.T.: Nonlinear Oscillations. Wiley, New York (1979)
2. Vlasov, V.Z.: Thin-Walled Elastic Beams, French translation: Pie‘ces longues en voiles minces. Eyrolles, Moscow (1962)
3. Loughlan, J., Ata, M.: The behavior of open and closed section carbon fiber composite beams subjected to constrained torsion. Compos. Struct. **38**, 631–647 (1997)
4. Ferrero, J.F., Barrau, J.J., Segura, J.M., Castanie, B., Sudre, M.: Torsion of thin-walled composite beams with midplane symmetry. Compos. Struct. **54**, 111–120 (2001)
5. Trahair, N.S., Bradford, M.A., Nethercot, D.A.: The Behavior and Design of Steel Structures to BS5950, 3rd edn. Spon Press, London (2001)
6. Salim, H.A., Davalos, J.F.: Torsion of open and closed thin-walled laminated composite sections. J. Compos. Mater. **39**(6), 497–524 (2005)
7. Shin, D.K., Kim, N.: Torsional analysis of thin-walled composite beams with single- and double-celled sections. Eng. Struct. **31**(7), 1509–1521 (2009)
8. Liu, K.C., Friend, J., Yeo, L.: The axial-torsional vibration of pretwisted beams. J. Sound Vib. **321**, 115–136 (2009)
9. Pi, Y.L., Trahair, N.S.: Inelastic torsion of steel I-beams. J. Struct. Eng. ASCE **121**(4), 609–620 (1995)
10. Trahair, N.S. (2003) Non-linear elastic non-uniform torsion. Research report no. R828. Department of Civil Engineering, The University of Sydney
11. Pi, Y.L., Bradford, M.A., Uy, B.: A spatially curved-beam element with warping and Wagner effects. Int. J. Numer. Methods Eng. **63**, 1342–1369 (2005)
12. Mohri, F., Damil, N., Ferry, M.P.: Large torsion finite element model for thin-walled beams. Comput. Struct. **86**, 671–683 (2008)
13. Cullimore, M.S.G.: The shortening effect, a nonlinear feature of pure torsion. In: Engineering structures. Academic Press, New York, pp 153–164 (1949)
14. Sapountzakis, E.J., Tsipiras, V.J.: Nonlinear nonuniform vibrations of bars by the boundary element method. J. Sound Vib. **329**(10), 1853–1874 (2010)
15. Sapountzakis, E.J., Tsipiras, V.J.: Shear deformable bars of doubly symmetrical cross section under nonlinear nonuniform torsional vibrations—application to torsional postbuckling configuration and primary resonance excitations. Nonlinear Dyn. **62**, 967–987 (2010)
16. Gregory, M.: Elastic torsion of members of thin open cross section. Aust. J. Appl. Sci. **12**, 174–193 (1961)

17. Ghobarah, A.A., Tso, W.K.: A non-linear thin-walled beam theory. Int. J. Mech. Sci. **13**(12), 1025–1038 (1971)
18. Tso, W.K., Ghobarah, A.A.: Nonlinear nonuniform torsion of thin-walled beams. Int. J. Mech. Sci. **13**(12), 1039–1047 (1971)
19. Rao, C.K.: Nonlinear torsional vibrations of thin-walled beams of open section. ASME Trans. Ser. E-J. Appl. Mech. **42**, 240–242 (1975)
20. Rosen, A.: Theoretical and experimental investigation of the nonlinear torsion and extension of initially twisted bars. ASME Trans. J. Appl. Mech. **50**, 321–326 (1983)
21. Rozmarynowski, B., Szymczak, C.: Non-linear free torsional vibrations of thin-walled beams with bisymmetric cross-section. J. Sound Vib. **97**, 145–152 (1984)
22. Attard, M.M.: Nonlinear theory of non-uniform torsion of thin-walled open beams. Thin-Walled Struct. **4**(2), 101–134 (1986)
23. Attard, M.M.: Nonlinear shortening and bending effect under pure torque of thin-walled open beams. Thin-Walled Struct. **4**(3), 165–177 (1986)
24. Mohri, F., Azrar, L., Potier-Ferry, M.: Flexural-torsional post-buckling analysis of thin-walled elements with open sections. Thin-Walled Struct. **39**, 907–938 (2001)
25. Saadé, K., Espion, B., Warzée, G.: Non-uniform torsional behavior and stability of thin-walled elastic beams with arbitrary cross sections. Thin-Walled Struct. **42**, 857–881 (2004)
26. Campanile, L.F., Thwapiah, G.: A non-linear theory of torsional divergence. Proc. Inst. Mech. Eng. Part C J. Mech. Eng. Sci. **223**(11), 2707–2711 (2009)
27. Sapountzakis, E.J., Tsipiras, V.J.: Effect of axial restraint in composite bars under nonlinear inelastic uniform torsion by BEM. Eng. Struct. **31**, 1190–1203 (2009)
28. Librescu, L., Song, O.: Thin-Walled Composite Beams: Theory and Application. Springer, Berlin (2006)
29. Malatkar, P.: Nonlinear vibrations of cantilever beams and plates. Ph.D. thesis, Virginia Polytechnic Institute and State University (2003)
30. Lacarbonara, W., Rega, G.: Resonant non-linear normal modes. Part II: activation/orthogonality conditions for shallow structural systems. Int. J. Non-Linear Mech. **38**, 873–887 (2003)